Subpicosecond Double Electron Bunch Generation

W. D. Kimura*, V. E. Yakimenko†, M. Babzien†, X. Ding‡, E. Kallos,§ K. P. Kusche†, I. V. Pavlishin†, I. V. Pogorelsky†, D. Stolyarov†, and F. Zhou¶

*STI Optronics, Inc., Bellevue, WA 98004 USA

†Brookhaven National Laboratory, Upton, NY 11973, USA

‡UCLA, Los Angeles, CA 90095, USA

§University of Southern California, CA 90089, USA

¶Stanford Linear Accelerator Center, Stanford, CA 94025, USA

Abstract. We have demonstrated creating two compressed electron beam bunches from a single 60-MeV bunch. Measurements indicate they have comparable bunch lengths (~100-200 fs) and are separated in energy by ~1.8 MeV with the higher-energy bunch preceding the lower-energy bunch by 0.5-1 ps. A possible explanation for the double-bunch formation process is also presented.

Keywords: Electron bunch, chicane, compression.
PACS: 41.75.Ht, 41.85.Ct, 29.27.-a

BACKGROUND

The Accelerator Test Facility (ATF) at Brookhaven National Laboratory (BNL) is performing various experiments related to advanced accelerator research. As part of these efforts, a chicane, designed and built by UCLA [1], was installed on the linac downstream of the RF accelerating structures. The chicane was designed to provide approximately 30 times compression of the incoming electron bunch. Figure 1 is a diagram and photograph of the chicane taken from [1].

It was discovered when compressing the electron bunch from the linac that the beam breaks up into two distinct bunches with subpicosecond compressed bunch lengths. It does this in a consistent and reliable manner. Unlike other facilities that are utilizing a chicane for pulse compression, the ATF does not have a subsequent RF acceleration section downstream of the chicane, which can be used to compensate for residual energy chirp on the electron beam (*e*-beam) exiting the chicane. As explained later, not being able to use a downstream acceleration section was one reason the double-bunch formation process was possible.

The remainder of this paper gives a possible explanation for this double-bunch formation and describes measurements for characterizing the double bunches.

Advanced Accelerator Concepts, AIP Conference Proceedings No. 877, M. Conde and C. Eyberger, eds., (American Institute of Physics, New York, 2006), pp. 527-533.

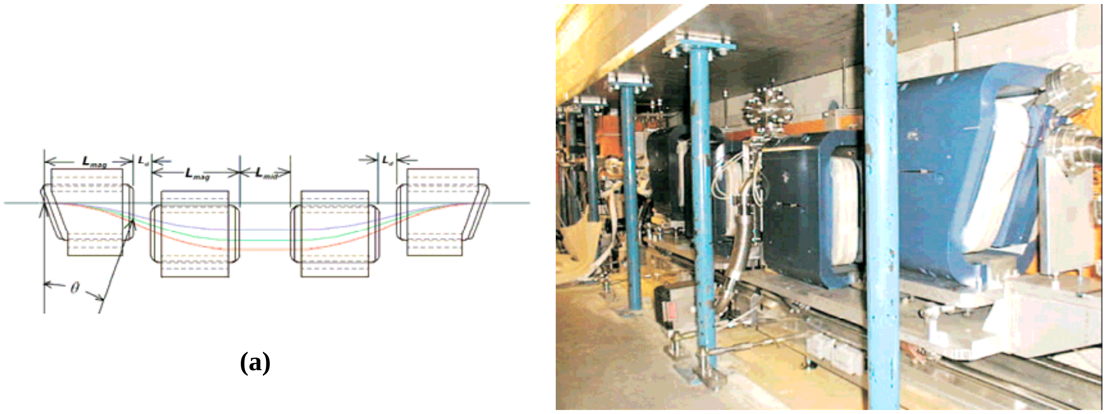

(a)

(b)

FIGURE 1. (a) Diagram of ATF chicane. (b) Photograph of chicane installed on ATF accelerator. (From [1]).

POSSIBLE EXPLANATION FOR DOUBLE BUNCH FORMATION

Our hypothesis is that the double-bunch formation is caused by the interaction between the chicane and the dogleg dipoles downstream of the chicane. Figure 2 is a cartoon illustrating one possible explanation for the double-bunch formation process. Drawn is the curvilinear pathway taken by the *e*-beam as it travels through the chicane and dogleg dipoles. Dipoles are indicated as rectangles. Ideally, the *e*-beam enters the chicane with a linear energy chirp as depicted by the dashed line in the energy-time graph drawn in the upper left-hand corner of Fig. 2. In reality, we believe the chirp is curved as shown in the graph. It is possible to identify two regions on this curve – Region 1, corresponding to electrons with a high amount of chirp, and Region 2, corresponding to electrons with a small amount of chirp. Note the Region 1 electrons precede the Region 2 electrons.

In passing through the first two dipoles of the chicane, electrons in Region 2 become compressed (we shall refer to these electrons as Bunch 2) and the electrons in Region 1 are not compressed yet (we shall call these electrons Bunch 1). In this middle section of the chicane, the beam is wide and, therefore, coherent synchrotron radiation (CSR) is weak. However, between the third and fourth chicane dipoles, the focus is tight and Bunch 1 experiences strong CSR effects. Consequently, after passing through the last dipole of the chicane, the Bunch 1 electrons finally are compressed, but now the Bunch 2 electrons become overcompressed. And, in the process of being overcompressed, the Bunch 2 electrons overtake in time the Bunch 1 electrons (see energy-time graph in middle-top of Fig. 2). Finally, the electrons pass through the dogleg dipoles where the beam is nominally focused to a tight spot. Now the strong CSR works on the Bunch 2 electrons to reduce their energy spread. The net result is a clean separation in energy and time between Bunches 1 and 2 as illustrated in the energy-time graph in the lower right-hand corner of Fig. 2.

Figure 3 shows energy spectrums of the *e*-beam at different positions along the pathway depicted in Fig. 2. Figure 3(a) is just before the chicane. The *e*-beam is a single bunch with an energy width of ~4% FWHM. Figure 3(b) is at the high-energy

Advanced Accelerator Concepts, AIP Conference Proceedings No. 877, M. Conde and C. Eyberger, eds., (American Institute of Physics, New York, 2006), pp. 527-533.

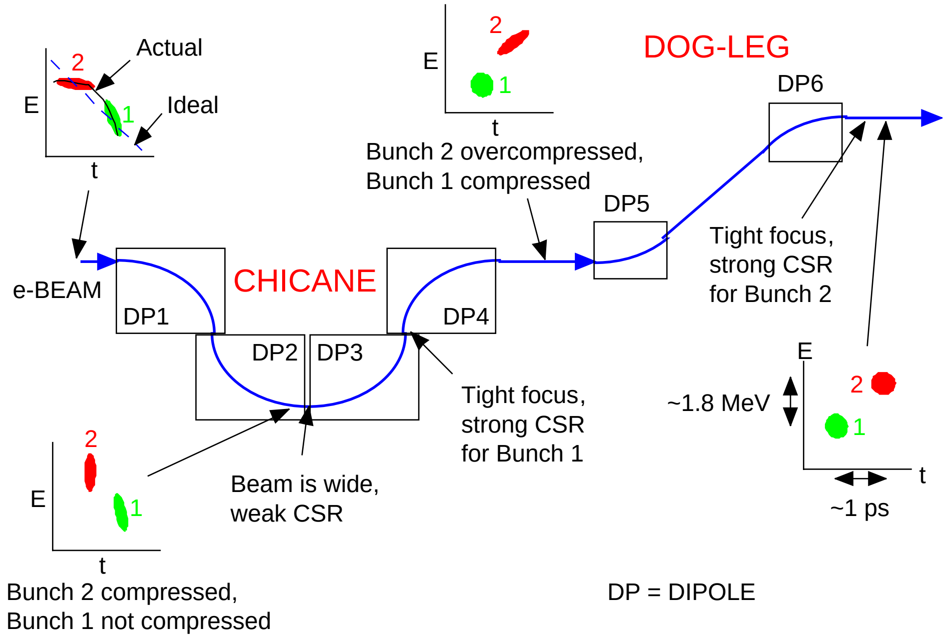

FIGURE 2. Cartoon of chicane/dogleg system showing a possible scenario for the double-bunch formation process.

slit located downstream of the chicane. It shows two distinct beams with, in this particular case, most of the charge in the lower-energy bunch (energy dispersion increases to the left in the images). Figure 3(c) is at the spectrometer at the end of the beamline. The two bunches are separated by approximately 1.8 MeV [see Fig. 5(a)].

We should emphasize that the preceding explanation is only a conjecture. We are in the process of performing ELEGANT modeling of the chicane/dogleg system in order to confirm our hypothesis and better understand this new phenomenon. Preliminary results of this analysis are given in Fig. 4. Figure 4(a) shows an example of the beam entering the chicane with a curved energy chirp. Figure 4(b) gives the resultant momentum-time distribution of the electrons after the dogleg. It is clear there has been a separation in energy of the electrons with a large group congregated in the lower half of the plot and a smaller group in the upper half. ELEGANT also indicates this separation in energy does not occur if CSR effects are turned off in the model.

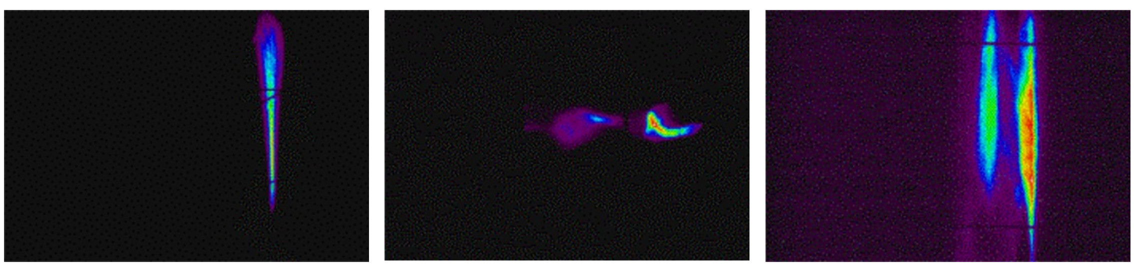

(a) **(b)** **(c)**

FIGURE 3. Raw energy spectrums of double-bunch *e*-beam. Energy dispersion increases to the left. (a) Before the chicane and without compression. Energy spread is ~4% FWHM. (b) At the high-energy slit located downstream of the chicane. (c) At the spectrometer at the end of the beamline.

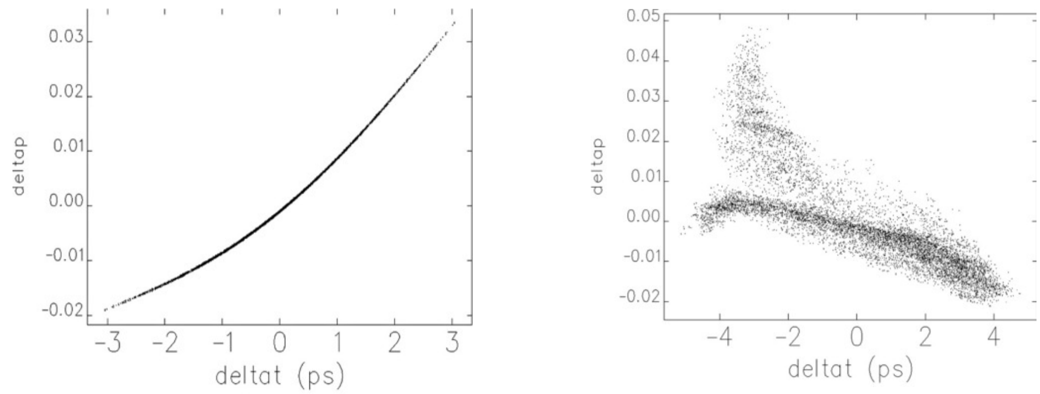

(a) **(b)**

FIGURE 4. Examples of output plots from ELEGANT of the chicane/dogleg system. (a) Momentum-time plot of electrons entering chicane. (b) Momentum-time plot of electrons at exit of dogleg.

It should be noted that we believe this double-bunch formation process would not have occurred if an *X*-band acceleration section had been installed downstream of the chicane to compensate for the energy chirp. Such an additional acceleration section has been used in other facilities with a chicane, such as SLAC.

CHARACTERIZATION OF DOUBLE BUNCH BEAM

Figure 5 shows energy spectrums of the double-bunch beam. Figure 5(a) is a single shot showing the two bunches separated in energy by 1.8 MeV. For the sake of identification we have labeled one bunch as the "high-energy (high-E) seed" and the other bunch as the "low-energy (low-E) seed." Figure 5(b) is an overlay of three shots taken many minutes apart. The good reproducibility of the spectrums indicates the energy distribution and positions are very stable.

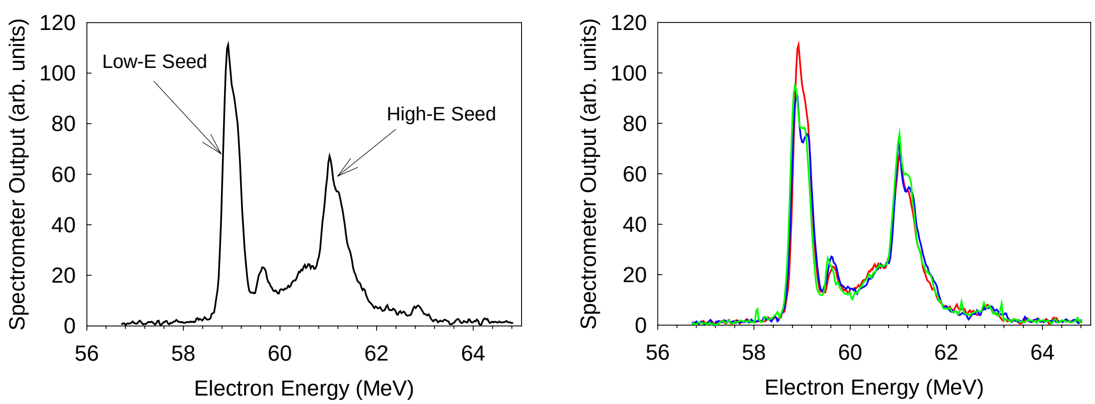

(a) **(b)**

FIGURE 5. Energy spectrums of double-bunch *e*-beam. (a) Typical single shot spectrum for the case when both bunches have comparable charge. (b) Three spectrums taken many minutes apart demonstrating stability of the double-bunch formation process.

Advanced Accelerator Concepts, AIP Conference Proceedings No. 877, M. Conde and C. Eyberger, eds., (American Institute of Physics, New York, 2006), pp. 527-533.

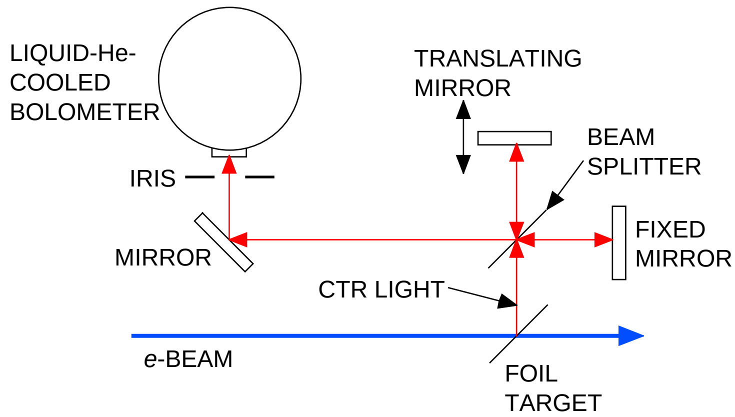

FIGURE 6. Schematic diagram of CTR interferometer.

A coherent transition radiation (CTR) interferometer was used to characterize the ATF compressed *e*-beam. Figure 6 shows a schematic diagram of the CTR interferometer system. The CTR emission is in the THz range. An autocorrelation of the CTR signal is obtained by scanning the translation mirror shown in Fig. 6.

Analysis of this autocorrelation signal yields information about the *e*-beam bunch characteristics [2]. Figure 7 shows two examples of the autocorrelation data and the curve fits derived from the autocorrelation integrals for the case of a single bunch and the double-bunches. Single bunch data was obtained by using the high-energy slit located downstream of the chicane to block one of the bunches (either the low-E or high-E bunch).

For a single bunch, the curve fit of the autocorrelation integral with the data requires selecting values for the bunch length and the cut-off frequency of the detection system, where we have assumed a Gaussian bunch shape. In particular, the

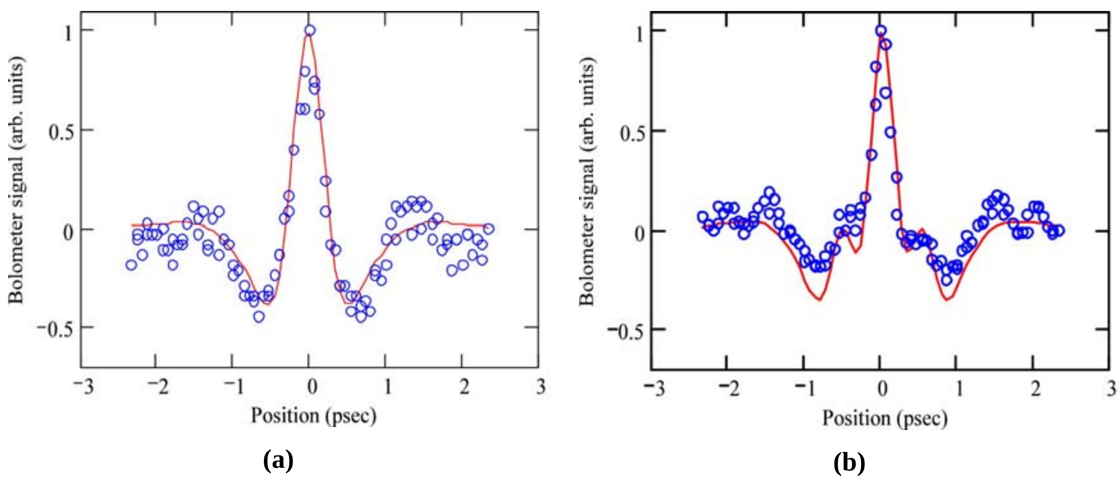

FIGURE 7. Example of raw data from CTR interferometer (circles) and the curve fits to the data (solid line) calculated from the autocorrelation integral [2]. (a) Single bunch. (b) Double bunches.

Advanced Accelerator Concepts, AIP Conference Proceedings No. 877, M. Conde and C. Eyberger, eds., (American Institute of Physics, New York, 2006), pp. 527-533.

width of the central peak of the autocorrelation signal is primarily affected by the bunch length. The shape of the curve on either side of the peak is mostly affected by the cut-off frequency. For the curve fit shown in Fig. 7(a), we find the bunch length is 144 fs and the cut-off frequency is 1.7 THz.

For a double *e*-beam bunch, there are five free parameters in the autocorrelation integral. Using CTR and beam position monitor (BPM) data for each bunch of the double bunches permits reducing the number of free parameters to two, i.e., the time delay between the two bunches and the cut-off frequency. For the example shown in Fig. 7(b), the single-bunch CTR data indicates the lengths of the two bunches is 144 and 90 fs, and the BPM data indicates the second bunch has 60% of the charge in the first bunch. Hence, for the curve fit shown in Fig. 7(b), we find the time delay between the bunches is 500 fs and the cut-off frequency is 1.8 THz.

DISCUSSION

Depending on the *e*-beam tune through the chicane and dipoles, the specific characteristics of the double bunches can be varied. For example, it is possible to have comparable charge in each bunch or a large difference in the charge ratio (e.g., 3:1). However, once the tune is set, the double-bunch beam characteristics are relatively stable as demonstrated in Fig. 5(b).

One important piece of information the preceding measurements could not indicate was whether the high-E bunch in Fig. 2 does indeed overtake in time the low-E bunch. To answer this question we took advantage of existing experimental apparatus installed at the ATF for the Staged Electron Laser Acceleration – Laser Wakefield (STELLA-LW) [3] experiment. STELLA-LW intends to use a compressed *e*-beam bunch to act as a seed in a capillary discharge plasma in order to generate a wakefield. This wakefield is then amplified by the ATF CO_2 laser pulse in a process called seeded self-modulated laser wakefield acceleration (SM-LWFA) [4].

Before performing the SM-LWFA experiment, preliminary plasma wakefield acceleration (PWFA) experiments were performed using the double-bunch beam. The results are discussed elsewhere in these proceedings [3] and are briefly reviewed here.

Each ~100-fs long bunch of the double-bunches is capable of generating wakefields. In doing so the electrons must lose energy. Moreover, the amplitude of the linear wakefield excited by a single bunch is expected to increase with plasma density as long as the plasma wavelength is shorter than the bunch length. In the PWFA tests, the energy spectrums of the double-bunches were taken as a function of the plasma density by delaying when the bunches entered the capillary discharge after the discharge was ignited.

It was found that the amount of energy loss for the high-E bunch increased as the plasma density increased even with the low-E bunch present. However, this was not true for the low-E bunch. When the high-E bunch was present, the low-E bunch tended to have a peak in its energy loss curve as a function of plasma density. In other words, the energy loss for the low-E bunch actually decreased at higher plasma densities. The fact the high-E bunch was contributing to this effect was confirmed by sending the low-E bunch through the plasma by itself. In this situation, the low-E bunch energy loss behavior was very similar to the high-E bunch, both in the amount

Advanced Accelerator Concepts, AIP Conference Proceedings No. 877, M. Conde and C. Eyberger, eds., (American Institute of Physics, New York, 2006), pp. 527-533.

and rate of loss. Put another way, the energy loss behavior of the high-E bunch when traveling with the low-E bunch is essentially the same as the low-E bunch when it travels alone through the plasma. Ergo, we can conclude that the high-E bunch must be preceding the low-E bunch since its energy loss behavior is as if it were traveling alone through the plasma. This conclusion is further supported by the fact the energy loss behavior of the low-E bunch is affected by whether the high-E bunch is present or not, implying that the wakefield produced by the high-E bunch is affecting how well the low-E bunch is able to couple energy into the plasma.

CONCLUSIONS

A novel method for generating a pair of subpicosecond electron bunches has been demonstrated. This method might be of interest in certain applications. For example, it may be possible to adapt this process in energy-doubling experiments where one bunch loses energy to accelerate the other bunch. However, instead of the accelerated bunch suffering a large energy spread while being accelerated, the decelerated bunch can endure the large energy spread thereby enabling the accelerated bunch to maintain a narrow energy spread.

ACKNOWLEDGMENTS

The authors wish to thank Dr. Patric Muggli for his helpful comments and the ATF staff for their assistance. This work was supported by the U.S. Department of Energy, Grant Nos. DE-FG02-04ER41294, DE-AC02-98CH10886, DE-FG03-92ER40695, and DE-FG02-92ER40745.

REFERENCES

1. R. B. Agustsson, UCLA, M.S. thesis, 2004.
2. A. Murokh, *et al*., Nucl. Inst. Meth. Phys. Res., A **410**, 452 (1998).
3. W. D. Kimura, *et al*., "Update on Seeded SM-LWFA and Pseudo-Resonant LWFA Experiments – (STELLA-LW)," in these proceedings.
4. N. E. Andreev, S. V. Kuznetsov, A. A. Pogosova, L. C. Steinhauer, and W. D. Kimura, Phys. Rev. ST Accel. Beams **9**, 031303 (2006).